NANO LETTERS

Letter

pubs.acs.org/NanoLett

Mechanically Durable and Highly Conductive Elastomeric Composites from Long Single-Walled Carbon Nanotubes Mimicking the Chain Structure of Polymers

Seisuke Ata,[‡] Kazufumi Kobashi,[†] Motoo Yumura,[†] and Kenji Hata*[,†,‡,§]

[†]Nanotube Research Center, National Institute of Advanced Industrial Science and Technology (AIST), 1-1-1 Higashi, Tsukuba, Ibaraki 305-8565, Japan

[‡]Technology Research Association for Single Wall Carbon Nanotubes (TASC), 1-1-1 Higashi, Tsukuba, Ibaraki 305-8565, Japan

[§]Japan Science and Technology Agency (JST), Honcho 4-1-8, Kawaguchi 332-0012, Japan

Supporting Information

ABSTRACT: By using long single-walled carbon nanotubes (SWNTs) as a filler possessing the highest aspect ratio and small diameter, we mimicked the chain structure of polymers in the matrix and realized a highly conductive elastomeric composite (30 S/cm) with an excellent mechanical durability (4500 strain cycles until failure), far superior to any other reported conductive elastomers. This exceptional mechanical durability was explained by the ability of long and traversing SWNTs to deform in concert with the elastomer with minimum stress concentration at their interfaces. The conductivity was sufficient to operate many active electronics components, and thus this material would be useful for practical stretchable electronic devices.

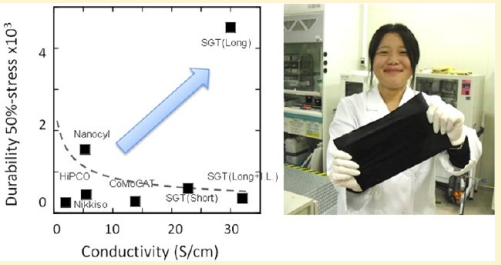

KEYWORDS: *Conductive rubber, mechanical durability, high conductivity, long single-walled carbon nanotube, fractal dimension*

A new and emerging paradigm for electronics is to integrate the attributes of flexibility and stretchability to realize soft and human-friendly applications, such as smart clothing, flexible displays, stretchable circuits, strain gauges, and implantable devices.[1−3] Stretchable, yet conductive materials are one of the fundamental issues for such devices, and thus intense effort has been invested to infuse electrical conductivity to stretchable elastomers by adding electrically conductive fillers.[4−6] Traditionally, carbon black and silver particles have been the filler of choice, and such elastomers composites have been widely used in various fields including electromagnetic shielding, seals, and electrostatic paints. The large aspect ratios, high electrical conductivity, and flexibility make carbon nanotubes (CNTs) candidates for fillers for conductive elastomers.[7−13] For example, Sekitani et al. developed a highly conductive rubber-like composite by mixing long single-wall nanotubes (SWNTs), an ionic liquid, and a fluoridated copolymer.[14] Kozolov et al. prepared highly elastic and conductive composites by the infiltration of vertically aligned MWNT forests with a polyurethane binder.[15] Albeit the conductivity was not exceptionally high (0.1−0.2 S/cm) because of the low loading level (0.1 wt %), the composite showed little degradation of the mechanical and electrical properties after 100 strain cycles.

On the basis of a literature survey, the intense effort to develop conducting elastomers has focused mainly on the conductivity aspect of elastomeric composites; however, for practical applications, mechanical durability is another fundamental requisite. Mechanical durability describes the ability of a material to bear many strain cycles and is, in fact, the most challenging requirement for conductive elastomers. This difficulty stems from the difference in Young's moduli between the fillers and elastomer matrix (filler Young's modulus being higher); therefore, when the conductive elastomer is strained, the relatively rigid fillers cannot completely follow the deformation of the elastomer. This difference in the Young's modulus induces stress concentration at the points along the interface between the filler and elastomer leading to structural distortion. Such structural distortions gradually accumulate with repeated strain cycles and eventually lead to the mechanical deterioration of the material and finally mechanical failure. For the elastomeric composites described above, in order to improve the durability, structural engineering was applied to the composites to create a net-shaped structure and coating it with polydimethylsiloxane (PDMS) or, in the case of the thin infiltrated MWNT forest (50 μm thick), lamination with a thin elastomeric support (200 μm thickness). As shown by these examples, to our knowledge, no elastomeric conductive composite have been able to maintain mechanical and electrical properties over extended strain cycling.

To address this issue, we explored the use of long SWNTs to mimic the chain structure of polymers and thereby achieved a

Received: November 30, 2011
Revised: March 26, 2012
Published: April 30, 2012

   dx.doi.org/10.1021/nl204221y | *Nano Lett.* 2012, 12, 2710−2716

highly conductive elastomeric composite (30 S/cm) with excellent mechanical durability (4500 strain cycles to failure). Our structural observation and analysis indicated that the excellent mechanical durability originated from the ability of long and traversing SWNTs to deform in concert with the elastomer matrix and thus minimize stress concentration between the two.

In this work, we used vertically aligned SWNTs (forests) synthesized by water-assisted chemical vapor deposition,[16] denoted as "supergrowth" (SG), to achieve long SWNTs. Millimeter-scale height SWNT (SG-SWNT) forests (Figure 1a) were synthesized from iron catalyst nanoparticles on a Ni alloy metal substrate[17] using ethylene and water. SG-SWNT forests satisfied many fundamental criteria as ideal fillers. First, the SWNTs were very long and thus had an exceptionally high aspect ratio. Second, SWNTs were not heavily bundled and easy to disperse because they were grown from isolated catalysts and only occupied ~3% of the forest volume. Third, SG-SWNTs exhibited the highest reported specific surface area (1000 m^2/g) for closed capped CNTs, an important point to create a large interfacial area between the SWNT filler and matrix for composites. These SWNT forests were removed from the growth substrate and suspended (0.3 wt %) in methyl isobutyl ketone (MIBK) by a high-pressure jet-milling homogenizer (60 MPa, nanojet pal, JN10, Jokoh) (Figure 1a). Jet milling exfoliates materials by ejecting suspensions through a nozzle and possesses a significant advantage over other dispersion methods, such as supersonication, to suspend long SWNTs with minimal shortening effects. From this suspension, SG-SWNT (10 wt %) elastomer composites were fabricated by adding fluorinated rubber (Daikin, Daiel-G912), stirring (25 °C for 16 h), casting, and finally drying (80 °C for 6 h). It should be noted that fluorinated rubber was chosen for comparison with previous work as well as being the choice for device integration because of its lack of impurities. As the fabrication process was scalable, we could easily fabricate large scale films with excellent uniformity as demonstrated by the A4-size (20 × 30 cm) composite sheet (Figure 1b). For comparison, by the same fabrication process, CNT/elastomer composites were fabricated from commercially available CNTs including CoMoCAT SWNTs (diameter 1.0 nm, length 1.0 μm), Nikkiso (>30 walls, size 10−30 nm, length 10−20 μm), HiPCO SWNTs (size 1.0 nm, length 100−1000 nm) and Nanocyl (~5 walls, size 15 nm, length 50 μm), and SG-SWNTs with ionic liquids. In addition, to address to the effect of length, a CNT/elastomer composite was made from SG-SWNTs treated with supersonication to cut the CNTs.

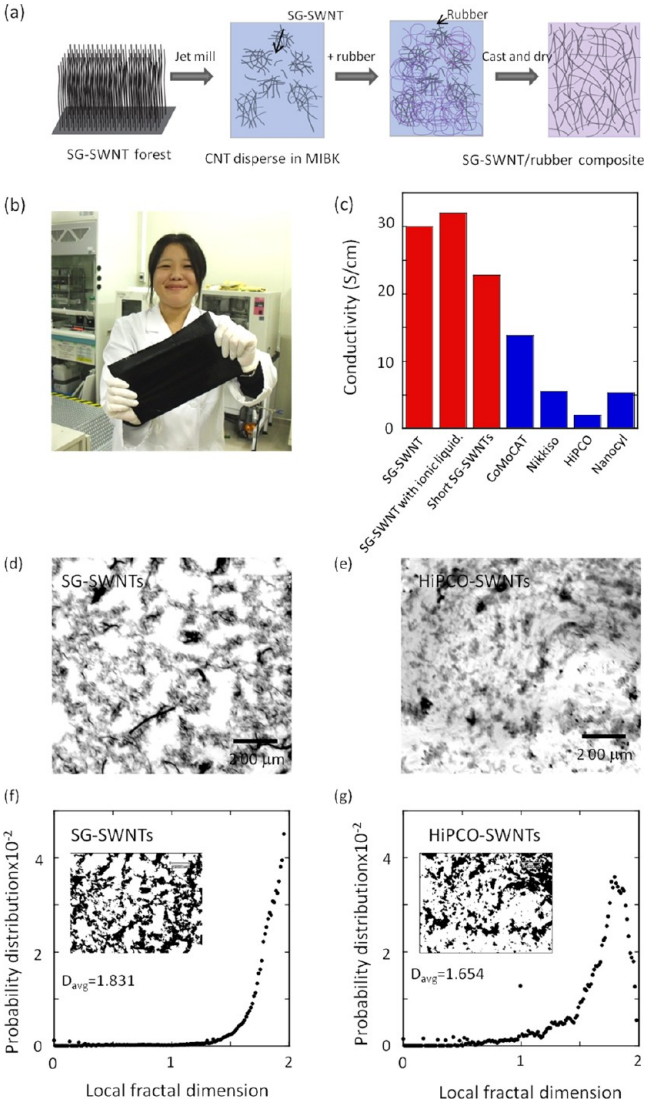

Figure 1. (a) Key steps in fabricating the SG-SWNT/rubber composite. (b) Photograph of the A-4 paper size SG-SWNT/fluorinated rubber film. (c) Conductivity of fluorinated rubber with various CNTs. Red bars means SG-SWNTs composites, and blue bars indicate composites with other CNTs. (d, e) Optical microscope images of the 1 wt % SG-SWNT and HiPCo with fluorinated rubber ultrathin section prepared with cryo-microstorming. (f, g) Calculated local fractal dimension versus frequencies from (d) and (e) by ImageJ Flac lac software.

The conductivities (Figure 1c) of the CNT/elastomer composites measured by a four-point probe electrical tester showed that SG-SWNTs provided superior conductivities (24−32 S/cm) than other CNTs (2−14 S/cm). The highest conductivity (32 S/cm) was obtained with ionic liquid; however, a comparable value (30 S/cm) was achieved from composites made solely from SG-SWNTs and rubber. While this conductivity is slightly lower than the highest value reported for SG-SWNT rubber composites with ionic liquids,[14,18] it is still ~30 times higher than other reported values for CNT/rubber composites[19,21] and is 300 000 times that of carbon black composites with the same loading level.[22,23] This level of conductivity is sufficient to drive active electronic components, such as organic transistors,[14] and thus we think this material is useful for flexible and stretchable electronics.

The origin of the high conductivity of SGT−rubber composites was investigated by internal structural observation and fractal dimension analysis. Composites (1 wt % SGT-SWNT and 1 wt % HiPCO) were sliced into very thin films (5 μm thickness) by a cryo-microtome and observed by an optical microscope (Figure 1d,e). The low level loading as well as the fabrication of a very thin film enabled to observe the CNTs embedded in the matrix. The SG-SWNTs formed a fibrous structure interconnected to each other, making a long-ranged closed cellular foam network that resembled foam of soap bubbles. In contrast, the HiPCO nanotubes tended to aggregate into isolated spherical particles. Clearly, the former structure would be preferred for high conductivity.

We analyzed the fractal dimension of the CNTs within the matrix to quantitatively characterize the CNT structure. The

dx.doi.org/10.1021/nl204221y | Nano Lett. 2012, 12, 2710−2716

fractal dimension, when applied to a composite filler, is a statistical quantity that indicates how completely the filler spans the matrix space and was calculated (ImageJ-FlaxLac_2,5) from two-dimensional binary black and white images (inset of Figure 1f,g) made from the optical images (Figure 1d,e). It should be noted that in two dimensions a fractal dimension of two corresponds to the maximum fractal dimension for a filler which completely spans the matrix space, while a fractal dimension of one corresponds to a straight line in the matrix space. We calculated the average fractal dimension for SG-SWNT and HiPco rubber composites using the box-counting method[24] by first constructing probability distributions of the local fractal dimensions for both rubber composites. The probability distributions of the local fractal dimensions for SG-SWNT and HiPco rubbers composites showed very different behavior. While the probability distribution of the SG-SWNT composite monotonically increased up to the local fractal dimension of two (Figure 1g), the probability distribution of HiPco composite peaked at 1.78 followed by a sharp drop with increasing fractal dimension (Figure 1f). This meant that the SG-SWNTs formed a longer-ranged network compared to HiPco SWNTs. From the probability distributions, the average fractal dimensions of the SG-SWNT and HiPCO rubber composites were calculated as 1.831 and 1.654, respectively. It is important to note that the fractal dimension of a random cluster system with an infinitely long continuous path is 1.895, which is very close to the average value for the SG-SWNT composite.[25] However, the average fractal dimension of the HiPCO composite physically corresponded to a structure midway between one and two dimensions. This meant that the SG−SWNTs formed a much long-ranged and continuous network than the HiPCO SWNTs, which was interpreted as the origin of superior conductivity of the SG-SWNTs rubber composite.

To investigate the influence of strain on conductivity, SG-SWNT and HiPCO (for comparison) rubber composites (10 wt %) were exposed to 100 loading−unloading strain cycles at 10% while monitoring the resistance. The resistance normalized to the initial value at 0% strain showed a relatively unvarying resistance of the SG-SWNTs composite (variation less than 20%) in this stress range when compared to previous reports of conducting polymers.[26,27] A very small hysteresis was observed between the loading and unloading phases, and the resistance returned to the initial value. These results were indication of very small material degradation. Even after 100 stress cycles, the change in the resistance remained 20% (Figure 2a). In contrast, the behavior of HiPCO/rubber composite exhibited highly different character; i.e., the resistance increased with stress (Figure 2b), hysteresis was observed between the loading and unloading phases, and the resistance steadily and monotonically increased with each stress cycle. After 100 strain cycles, the resistance increased nearly 8 times of the initial value. Such behavior is commonly observed for conventional conductive rubbers and is indication of material deterioration. These results clearly demonstrated that SG−SWNTs are superior fillers for mechanically durable composites.

Further tests were implemented to test to the mechanical durability of the CNT/rubber composites. Stress−strain curves showed that the maximum strain gradually decreased with strain cycles (Figure 3a). This is a generally observed

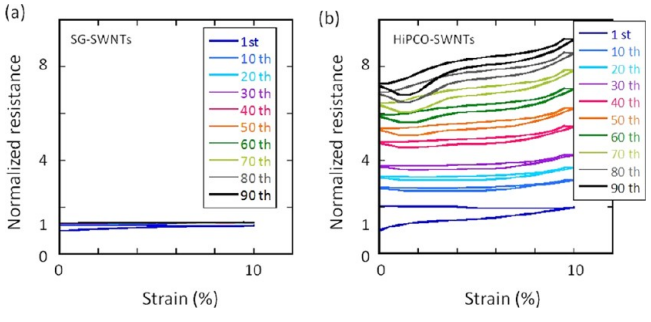

Figure 2. (a, b) Normalized resistance change versus strain of SG-SWNT (a) and HiPCO (b) rubber under repeating 10% strain. Each line corresponds to 1, 10, 20, 30, 40, 50, 60, 70, 80, and 90 cycles.

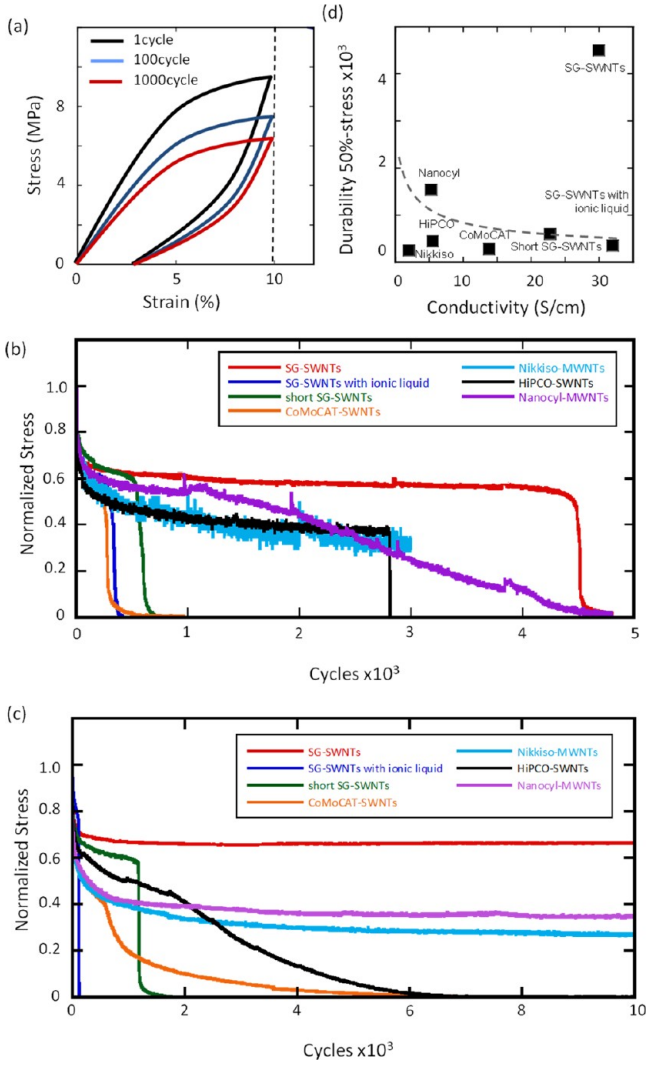

Figure 3. (a) Strain recovery curves for SG-SWNTs fluorinated composite with increasing number of cycles during mechanical durability test. (b, c) Normalized stress versus cycles at strain 10% (b) and 5% (c) on SG-SWNTs (red line), SG-SWNT with ionic liquid (blue line), short SG-SWNTs (green line), CoMoCAT (orange line), Nikkiso (light blue line), HiPCO (black line), and Nanocyl (purple line) composites. Cycle frequency was 0.25 Hz. This value was chosen to match the deformation relaxation of SG-SWNT/fluorinated rubber composite. At higher cycle frequency (1 Hz), the rate of the deformation relaxation was longer than the cycle rate and therefore not comparable. (d) Conductivity versus durability map for various conductive composites.

dx.doi.org/10.1021/nl204221y | Nano Lett. 2012, 12, 2710−2716

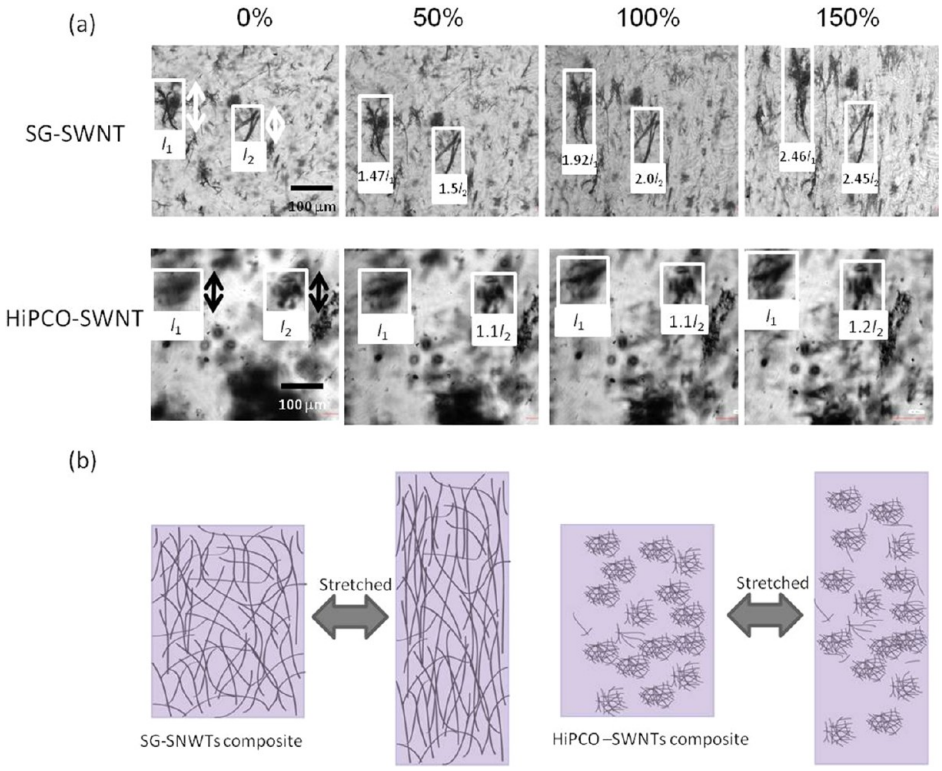

Figure 4. (a) Morphology of SG-SWNTs and HiPCO-SWNTs under strain. (b) Model of the CNTs network structure in composites under deformation. SG-SWNTs maintain their contacts under deformed matrix as their high aspect ratio (left). However, aggregated CNTs, such as HiPCO-SWNTs, lose contact with each other (right).

phenomenon and reflects the softening of the elastomer caused by progressive deformation of the material initiated by stress concentration in the toughest regions. To address this point, mechanical durability tests were implemented on CNT/ composites. Fillers investigated included SG-SWNTs, SG-SWNT with ionic liquid, short SG-SWNTs, CoMoCAT and HiPCO SWNTs, Nikkiso, and Nanocyl-MWNTs (Figure 3b). For these composites, the normalized maximum stresses were plotted against the number of cyclic tests required to reach the fatigue limit. Importantly, the SG−SWNT filler (blue line in Figure 3b) showed a very different and peculiar trend from other fillers. During the initial aging stage, the normalized stress quickly reduced to 0.6 within 400 cycles, similar to other fillers. However, after this aging stage, the normalized stress remained unchanged for the subsequent 4000 cycles. Within this stable period, the normalized stress only decreased for 10%. After 4500 cycles, the composite degraded and fractured. The number of cycles to failure of composites made from HiPCO SWNTs (black line in Figure 3b, 2800 cycles), Nikkiso (light blue line in Figure 3c, 2900 cycles), and Nanocyl MWNTs (purple line in Figure 3b, 4500 cycles) fillers also exceeded 1000 cycles; however, in contrast to the SG-SWNTs composite, the normalized stress monotonically decreased with each strain cycles. Among the fillers studied, plateauing of the normalized stress at 10% strain was only observed for the SG-SWNT fillers and stands alone in its character. It is clear that this plateauing is a critical advantage for practical use. Mechanical durability tests on these composites at a lower strain level of 5% showed a similar trend to that taken at 10%, and the SG-SWNT composite (red line in Figure 3c) showed the best performance. While SG-SWNT with ionic liquid (blue line in Figure 3c), short SG-SWNTs (green line in Figure 3c), CoMoCAT SWNTs (orange line in Figure 3c), and HiPCO SWNTs (black line in Figure 3c) composites fractured within 10^4 cycles, SG-SWNT, Nikkiso-MWNT (light blue line in Figure 3c), and Nanocyl-MWNT (purple line in Figure 3c) composite were stable up to 10^4 cycles. However, SG-SWNTs showed the minimum stress deviation (34%) compared to Nikkiso-MWNTs (75%) and Nanocyl-MWNTs (67%) composites.

Importantly, for SG-SWNTs with ionic liquid (blue line in Figure 3c,d) and short SG-SWNTs fillers (green line in Figure 3c,d), the composites quickly degraded and the numbers of cycles to failure were only 300 and 530, respectively, and much smaller than that of SG-SWNTs composite (red line in Figure 3c,d). These results were illustrative because it revealed that the use of SG-SWNTs itself did not necessary lead to increased mechanical durability. On the basis of these results, we propose that the length of CNTs is one of the crucial factors for excellent mechanical durability. In addition, this result demonstrates that although the use of ionic liquid is beneficial for higher conductivity, it leads to a degradation of the mechanical properties. For example, mechanical strain−stress curve (Supporting Information Figure S1) of SG-SWNT with ionic liquid composite showed lower mechanical failure strain level with increasing ionic liquid. Indeed, when ionic liquid is added, the SG-SWNTs composite is more like a paste than an elastomer, and thus in Sekitani's work the ionic liquid SWNT/ rubber composite was mounted on a separate elastomer for mechanical support.

A two-dimensional map (Figure 3d) of the conductivity versus mechanical durability (defined as the number of cycle when the strain decreases 50% from the initial value) of the CNT/rubber composites revealed an inverse relationship between the conductivity and mechanical durability. For

dx.doi.org/10.1021/nl204221y | *Nano Lett.* 2012, 12, 2710−2716

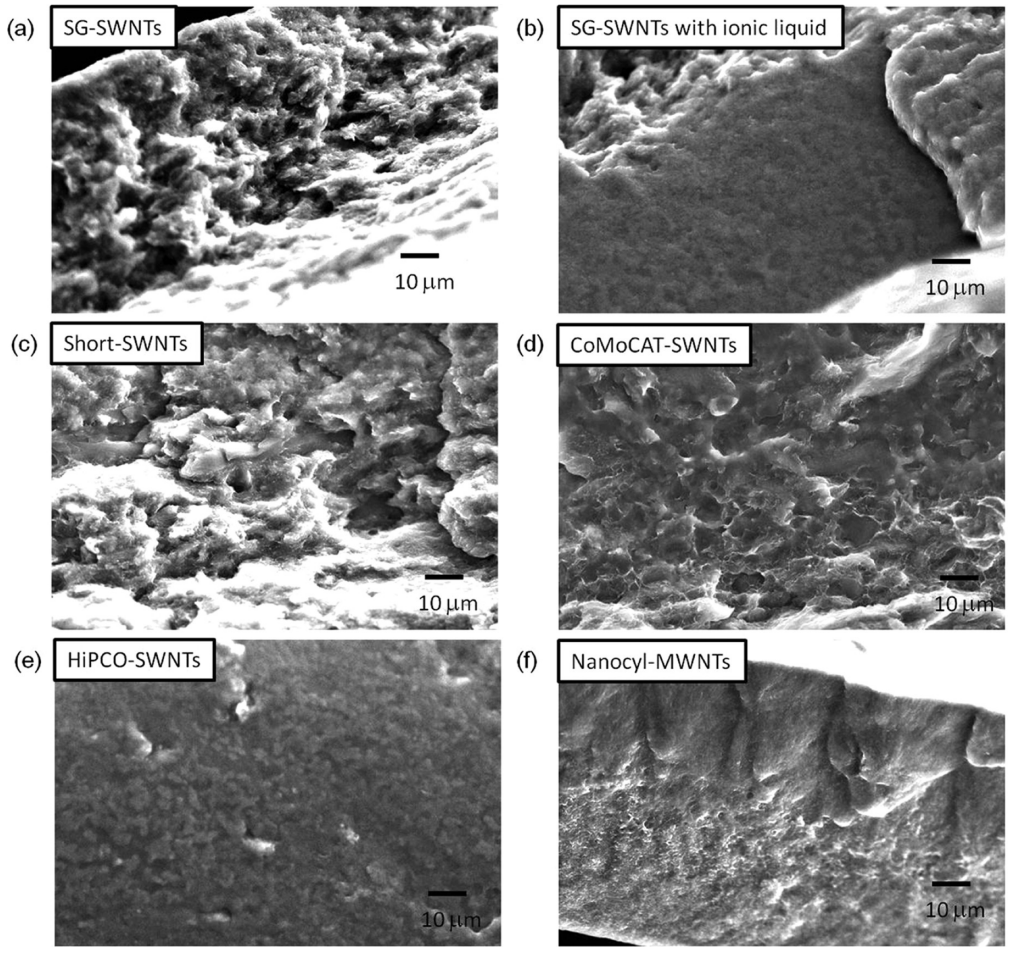

Figure 5. SEM images of cryo-fracture surfaces: (a) SG-SWNTs, (b) SG-SWNT with ionic liquid, (c) short SG-SWNT, (d) CoMoCAT-SWNTs, (e) HiPCO-SWNTs, (f) Nanocyl-MWNTs.

conductive fillers, high loading levels (>30 wt %), in general, provided higher conductivity. On the other hand, incorporation of high loading levels of fillers into the elastomers not only increased the stiffness of the resulting composite but also led to decreased mechanical durability. This simple picture readily described the trend observed in the map and demonstrated the fundamental difficulty in simultaneously achieving high conductivity and excellent mechanical durability. The SG-SWNT rubber composite formed a distinct and isolated point in the map and was the only example that broke this general trend.

To understand the origin of durability, we examined the structural changes in SG-SWNTs and HiPCO composites (Figure 4a) under different levels of strains by in-situ laser scanning microscopy. The structural distortions of the SG-SWNT and HiPCO CNT network with increased strain were followed as indicated by the boxes. As shown, the SG-SWNT network elongated along and proportional to the strain. For example, the feature marked in Figure 4a elongated 47%, 92%, and 146% times when strained at 50%, 100%, and 150%. In sharp contrast, the HiPCO spherical particles did not elongate much with the strain. For example, even when strained at 150%, the HiPCO particles only elongated 20%. We would like to note that these tests were implemented up to a strain level close to the fracture strain (170%) of the material. These results highlighted the exceptional ability of the SG-SWNTs to deform simultaneously with the matrix over a wide strain range. The long SG-SWNTs used in the work is a filler that has the highest aspect ratio (>10^6) with a very small diameter (~3 nm) and thus is a filler that most resembles the long-chain polymers in structure. Because of their similar structure, we interpret that the SG-SWNT would experience all of the stresses and strains imposed upon matrix itself and would react in a similar way. In this manner, although not stretchable itself, we expect that a traversing long SG−SWNT would easily flex (Figure 4b) in concert with the polymer molecules and thus deform with the elastomer with minimum stress concentration along the interface. We propose that this is mechanism of the excellent mechanical durability observed for SG-SWNTs.

Scanning electron microscope (SEM) images of the fracture surfaces of the CNT/rubber composites were investigated to address to the interaction between the CNT fillers and the rubber matrix. The composites (CNT 10 wt %) were immersed into liquid nitrogen, and the bending fractures were imaged by SEM (Figure 5a−f). While the SG-SWNT and SG-short composites showed a very rough surface, the surfaces of HiPCO-SWNTs, Nanocyl-MWNTs and SG-SWNTs with ionic liquid composites were very flat. In addition, while no bare CNTs were observed for the SG-SWNTs composite, Nanocyl and Nikkiso (Supporting Information Figure S2) composites showed many CNTs protruding from the surface. At material failure, crack propagation occurred at weak points within the composite. A flat fracture surface means that the crack propagated easily throughout the matrix without experiencing

dx.doi.org/10.1021/nl204221y | *Nano Lett.* 2012, 12, 2710−2716

variations in resistance. In addition, bare CNTs protruding from the surface means that the CNT failed to sustain and reinforce the surrounding rubber. These features indicate a weak interaction between the CNT fillers and the matrix.

On the other hand, when the CNTs have a strong affinity and interact strongly with the rubber, the CNTs would anchor the rubber and form strong segments. Such sections would not easily crack because the load applied to the matrix would be efficiently transferred to the CNTs, and thus the fracture surface would become rough with no bare CNTs exposed. We interpret that the high surface area of the SG-SWNTs provided a very large interfacial area and, therefore, a strong interface between the SG-SWNTs and the matrix. It is interesting to note that ionic liquid degraded the mechanical durability of the SG-SWNT composite. Since ionic liquid were used as compatibilizers,[28] they were expected to exist at the interface of the SG-SWNT and rubber. The flat fracture surface suggested that the ionic liquid at the interface greatly decreased the coupling between the filler and matrix resulting in a weak interface. As discussed, the results demonstrated the strong affinity between the SG-SWNTs and the matrix which created an interface capable of bearing heavy load transfer. These features are expected to provide superior mechanical durability, in agreement with the experimental observations.

In conclusion, we have successfully fabricated a highly conductive elastomeric composite (30 S/cm) with excellent mechanical durability. Our research demonstrated that the use of SWNT fillers that mimics long-chained polymers is the key to achieve excellent mechanical durability. When such SWNTs were dispersed into the matrix, they could easily deform in concert with the matrix with minimum stress concentration. We think that the mechanical durability can be further improved by various approaches including use of longer SWNTs, tailoring the defect density of SWNTs, development of dispersion processes to mix the long-SWNTs into the rubber matrix with minimum cutting, and better debundling. We believe that the present research demonstrated an approach to surmount the general problem of mechanical durability of conductive elastomers and thus represents a step forward for practical stretchable electronic devices.

Methods. *Materials.* Fluorinated rubber (Daiel-G912) is purchased from Daikin Co. CoMoCAT-SWNT, Nikkiso-MWNT, HiPCO-SWNT, and Nanocyl-MWNT are purchased from Southwest Nanotechnologies, Inc., Nikkiso Co., Unidym Inc., and Nanocyl s.a., respectively.

Structure Observation. Scanning electron microscopy (FE-SEM S-4800) was performed to observe the structures of cross sections of composites.

Conductivity Measurement. The conductivities of composites were measured with four-terminal method (MCP-T610, Mitsubishi Chemical Analytech Co., Ltd.).

Mechanical Durability Test. The tensile test samples were cut into a dog-bone shape from the sheet with dimensions of 40 mm (length) × 2.0 mm (width) × 0.04 mm (thickness). The extension rate and the gauge length were 30 mm/min and 20 mm. The tests were performed using a Micro Autograph MST-I (Shimadzu Co.) with 50 N load cell. The mechanical durability tests were in conformity to tensile mechanical durability test (standard protocol defined as JIS K7118). Frequency, temperature, wave profile, and maximum strain were set as 0.25 Hz, 25 °C, triangular wave, and 5%, respectively.

Box Counting. Box counting is a method to estimate the fractal dimension. A box counting fractal dimension D_0 is described as follows:

$$D_0 = \lim_{\varepsilon \to 0} \log N(\varepsilon)/\log(1/\varepsilon) \quad (1)$$

$N(\varepsilon)$ is defined as the minimum number of the grids that fully covers the object (e.g., CNT in optical image), ε being the edge length of the grid. Therefore, the box counting fractal dimension can be estimated by counting the number of grids which include object.

■ ASSOCIATED CONTENT

Supporting Information

Figures S1 and S2. This material is available free of charge via the Internet at http://pubs.acs.org.

■ AUTHOR INFORMATION

Corresponding Author

*E-mail kenji-hata@aist.go.jp; Tel +81-29-861-4654/+81-29-861-4851.

Notes

The authors declare no competing financial interest.

■ ACKNOWLEDGMENTS

We gratefully acknowledge Dr. Don N Futaba for useful discussions. Support by New Energy and Industrial Technology Development Organization is acknowledged.

■ REFERENCES

(1) Fabrice, A.; Schmitt, P. M.; Gehin, C.; Delhomme, G.; McAdams, E.; Dittmar, A. *Inf. Technol. Biomed.* **2005**, *9* (3), 325.
(2) Kim, D. H.; Ahn, J. H.; Choi, W. M.; Kim, H. S.; Kim, T. H.; Song, J.; Huang, T.; Liu, Z.; Lu, C.; Rogers, J. A. *Science* **2008**, *320*, 507.
(3) Gonzalez, M.; Axisa, F.; Bulcke, M. V.; Brosteaux, D.; van Develde, B.; van Fleteren, J. *Microelectron. Reliab.* **2008**, *48* (6), 825.
(4) Das, N. C.; Chaki, T. K.; Khastgir, D. *Polym. Int.* **2002**, *51* (2), 156.
(5) Das, N. C.; Chaki, T. K.; Khastgir, D. *Carbon* **2002**, *40* (6), 807.
(6) Mohanraj, G. T.; Chaki, T. K.; Chakraborty, A.; Khastgir, D. *J. Appl. Polym.* **2004**, *92* (4), 2179.
(7) Koerner, H.; Liu, W.; Alexander, M.; Mirau, P.; Dowty, H.; Vaia, R. A. *Polymer* **2005**, *46*, 4405.
(8) Li, Y.; Shimizu, H. *Macromolecules* **2009**, *42*, 2587.
(9) Bokobza, L. *Polymer* **2007**, *48* (17), 4907.
(10) Jiang, M. J.; Dang, Z. M.; Xu, H. P. *Appl. Phys. Lett.* **2006**, *89*, 182902.
(11) Suhr, J.; Koratkar, N.; Keblinski, P.; Ajayan, P. *Nat. Mater.* **2005**, *4*, 134.
(12) Jiang, M. J.; Dang, Z. M.; Xu, H. P. *Appl. Phys. Lett.* **2007**, *90* (4), 042914.
(13) Coleman, J. N.; Khan, U.; Blau, W. J.; Gun'ko, Y. K. *Carbon* **2006**, *44* (9), 1624.
(14) Sekitani, T.; Noguchi, Y.; Hata, K.; Fukushima, T.; Aida, T.; Someya, T. *Science* **2008**, *321*, 1468.
(15) Shin, M. K.; Oh, J.; Lima, M.; Kozolov, M. E.; Kim, S. J.; Baughman, R. H. *Adv. Mater.* **2010**, *22*, 2663.
(16) Hata, K.; Futaba, D. N.; Mizuno, K.; Namai, T.; Yumura, M.; Iijima, S. *Science* **2004**, *19*, 1362.
(17) Futaba, D. N.; Hata, K.; Namai, T.; Yamada, T.; Mizuno, K.; Hayamizu, Y.; Yumura, M.; Iijima, S. *J. Phys. Chem. B* **2006**, *110*, 8035.
(18) Das, A.; Stockelhunber, K. W.; Jurk, R.; Fritzsche, J.; Kluppel, M.; Heinrich, G. *Carbon* **2009**, *47*, 3313.
(19) Meincke, O.; Kaempfer, D.; Weickmann, H.; Friedrich, C.; Vathauer, M.; Warth, H. *Polymer* **2004**, *45*, 739.

(20) Das, A.; Stockelhuber, K. W.; Jurk, R.; Saphiannikova, M.; Fritzshe, J.; Lorenz, H.; Kluppel, M.; Heinrich, G. *Polymer* **2008**, *49*, 5276.
(21) Tsuchiya, K.; Sakai, A.; Nagaoka, T.; Uchida, K.; Furukawa, T.; Yajima, H. *Compos. Sci. Technol.* **2011**, *71*, 1098.
(22) Karasek, L.; Sumita, M. *J. Mater. Sci.* **1996**, *31*, 281.
(23) Sumita, M.; Sakata, K.; Asai, S.; Miyasaka, K.; Nakagawa, H. *Polym. Bull.* **1991**, *25*, 265.
(24) Foroutan-pour, K.; Dutilleul, P.; Smit, D. L. *Appl. Math. Comput.* **1999**, *105*, 195.
(25) Pietronero, L. *Fractals' Physical Origin and Properties*; Plenum Press: New York, 1989; pp 308−311252.
(26) Kim, T. A.; Kim, H. S.; Lee, S. S.; Park, M. *Carbon* **2012**, *50*, 444.
(27) Flandin, L.; Chang, A.; Nazarenko, S.; Hiltner, A.; Bear, E. *J. Appl. Polym. Sci.* **2000**, *76*, 894.
(28) Fukushima, T.; Kosaka, A.; Ishimura, Y.; Yamamoto, T.; Takigawa, T.; Ishii, N.; Aida, T. *Science* **2003**, *300*, 2072.